Annales de Chimie - Science des Matériaux
Vol. 49, No. 2, April, 2025, pp. 157-162
Journal homepage: http://iieta.org/journals/acsm

Optimization of Copper Oxide Nanoparticles Production by Pulsed Laser Ablation: A Study on Energy Density Effects

Ali M. Ahmed[1*], Russul M. Shehab[2], Mayss Alreem N. Hammed[2], Ghaidaa A. Khalid[2], Ghufran S. Jaber[3], Mustafa Adnan Zaidan[4]

[1] College of Medicine, Mustansiriyah University, Baghdad 10011, Iraq
[2] Electrical Engineering Technical College, Middle Technical University, Baghdad 10011, Iraq
[3] Remote Sensing College, Al Karkh University of Science, Baghdad 10011, Iraq
[4] Medical Technical College, Al-Farahidi University, Baghdad 10011, Iraq

Corresponding Author Email: ali.majeed@uomustansiriyah.edu.iq

https://doi.org/10.18280/acsm.490206

Received: 3 March 2025
Revised: 11 April 2025
Accepted: 15 April 2025
Available online: 30 April 2025

Keywords:
copper oxide, laser ablation, nanoparticles, optical properties, SEM

ABSTRACT

Nanomaterial's especially metal oxide nanoparticles have recently been of interest in many fields such as physics, biology, and medicine. This work employs Pulsed laser ablation in liquid as a clean and versatile technique for synthesizing copper oxide nanoparticles that produce high-quality materials with minimal chemical interference. Copper plates were treated in deionized water using laser energy density to produce copper nanoparticles at two different energy densities of 400 and 800 mJ. Copper oxide nanoparticles categorized by X-ray diffraction method, UV-visible spectroscopy and scanning electron microscopy (SEM). Changes in absorption spectra and subsequent UV-visible spectroscopy were observed for particle size, with a redshift at greater laser intensity (650 nm for 800 mJ compared to 600 nm for 400 mJ). X-ray diffraction (XRD) result presented this material as having a monoclinic crystalline structure with particle size estimated to be between 30 and 60 nm (34.626° and 34.714° 2θ for 400 mJ; 31.49° and 66.45° 2θ for 800 mJ). Specific morphological analyses through SEM showed products contained elongated nanoflake-like shaped particles extending to 800 mJ that aggregated into a rough structure which boost their catalytic effectiveness. These results confirm application for photocatalytic activities, antibacterial activity, and enhanced biomedical science by controlling size, optical, structure, and morphology.

1. INTRODUCTION

Nanomaterials are a significant category of materials used in creating new technologies in physics, biology, and medicine. It is much explored in different fields of applications today [1, 2].

One example is that, in physics, CuO nanoparticles are used in gas sensors and high-temperature superconductors due to their unique electricity. CuO is often utilized in biology to make antimicrobial coatings and aids in wound healing. CuO NPs, because of their high surface activity and biocompatibility, are used in medicine as drug carriers, anticancer agents, and contrast agents for imaging [3, 4]. In the past years, several researchers have synthesized and characterized metal oxide nanoparticles including copper oxide, and found enhanced biological and photocatalytic performance [5, 6]. CuO nanoparticles have attracted special focus among metal oxide nanoparticles because they are the simplest copper compounds with unique physical characteristics like high-temperate superconductivity and electron correlation [7-9]. Superconductivity at higher temperatures in CuO-based materials allows electricity to flow without resistance at those temperatures, helping both efficient power systems and strong magnets. CuO's magnetic and electronic behaviors that come from strong electron correlation make it a strong candidate for spintronic devices, memory storage, and advanced electronics. Thanks to their intrinsic properties and chemical stability, CuO nanoparticles are very versatile in modern technologies. The wide band gap (1.4 eV) and its high carrier mobility in CuO monoclinic crystal structure in C2/c space group make it suitable for visible light photocatalysis [10]. Whereas Cu_2O is not as stable under ambient conditions; CuO is more stable under the ambient conditions and resists oxidation during applications [11]. However, since CuO is responsive under visible light, the process becomes less expensive in terms of energy consumption in photocatalytic processes [12]. This study showed that metal oxide NPs such as ZnO, Fe_2O_3, Fe_3O_4, MgO, CuO, TiO_2, and SiO_2 have good antibacterial properties at low temperatures. This makes transition metal oxide nanoparticles even more attractive due to their outstanding antibacterial properties [13, 14]. There is evidence that CuO nanoparticles possess a very high impact as an anticancer and antioxidant agent and a drug transport system for biomedical research.

Studies have shown that CuO nanoparticles are toxic to cancer cells such as those from the breast and lung, and this happens through oxidative stress and apoptosis [9]. Mohammed et al. [15] reported that carbon-wrap CuO nanoparticles significantly decreased breast cancer cells proliferation in MCF-7 cells. Moreover, due to their strong surface activity, these NPs easily carry and release drugs properly, which suggests they are powerful drug delivery tools. These results show that CuO NPs have great potential to serve multiple purposes in treating cancer and diagnosing diseases [12].

Many different approaches have been used to create NPs. A prominent top-down method for producing almost any kind of material, including NP colloids with controlled size and shape, is pulsed laser ablation in liquids (PLAL) [15, 16]. This strategy has a benefit in that crystalline nanoparticles can be readily produced in one step, without contaminants or byproducts [17]. Laser ablation started as a research topic in the 1960s but has become much more effective and useful for creating nanoparticles thanks to more recent advances. The method is popular as it produces high-quality nanoparticles that are clean and contamination-free in only one step, without using any chemicals. With the help of ultrafast pulses, tunable wavelengths, and high repetition rates in laser systems, researchers can now manage particle size, shape, and distribution with great precision. In addition, PLAL is popular in both academia and industry because it is friendly to the environment, adjustable to many materials, and can be applied in healthcare [3]. The invention of the laser itself marked the beginning of research into laser ablation [18, 19]. In this method, however, liquids are confined and appropriate solid targets are selected for flexible design [20].

The initial step in using a laser pulse to target an object is to submerge it in liquid. In order for laser ablation to begin, an extremely hot environment must be established before electrons can absorb the energy of the laser pulse. After absorption, excited electrons transmit the energy to the crystal lattice heat up the laser-brightened area very quickly, and break it down, vaporizing the metal and solvent contacting with the laser-brightened area [21, 22].

The PLAL process can then activate various mechanisms such as the creation, modification, and condensation of plasma generated by a laser. The liquid limits the plasma plume's ability to expand, making the liquid the exciter of NPs nucleation and growth. The negatively charged nanoparticles should aggregate into stable colloids in the right media [23-26].

A nucleus's surface charge is a key modulator of its size and aggregation state [27]. In addition, the NPs are surrounded by the liquid molecules in a protective shell that prevents aggregation and increases durability [28]. As an instance, there are a number of laser parameters that can be fine-tuned to produce stable nanoparticles in small dispersions, such as focusing, pulse duration, repetition rate, wavelength, and fluence.

These lasers have blown the methods of processing and characterizing nanomaterials into further possibilities. This process has great advantages over the traditional methods which are enumerated below: This allows for the flexible adjustment of a huge number of input parameters for ablation, which determines a size, shape, and stoichiometry of the nanomaterial. Moreover, it enables the synthesis of nanomaterials with precise chemical composition as well as a surface that is not contaminated with chemical products [29]. Specifically, CuO nanomaterials have attracted considerable attention compared with all metal oxide nanomaterials due to their unique properties [30, 31].

Therefore, the synthesis of CuO with different sizes and shapes from pure copper foil, immersed in deionized water, is demonstrated using PLAL, a combination of physical and chemical processes. UV-visible spectroscopy was employed to characterize the synthesized colloidal nanoparticles. Moreover, the deposited thin films were characterized using XRD and FE-SEM scanning microscopy techniques [32, 33].

The size of the CuO nanoparticles was evaluated using XRD with the help of Scherrer's formula [34]. The objective of this paper is to optimize the optical and morphological properties of CuO nanoparticles prepared via PLAL according to laser energy density (400 and 800 mJ) and correlate them with photocatalytic and biomedical properties.

2. MATERIALS AND METHODS

Falcon Trading Company Faridkot, prepared samples by laser ablation utilizing the Picosecond laser (model: The Pharos laser, produced by Light Conversion in Lithuania, gives 100 ps pulses and has energy settings of 400 and 800 mJ [35].

The beam is focused by an objective onto a copper plate with a diameter of 2 cm. The target was set at the base of a 3mL glass container containing a little water Figure 1. Before each experiment, the copper plate was polished and the layer of DI water over the target was maintained at 12 mm deep. The vessel revolved at a constant speed each minute. Two samples were prepared using the arrangement in the image below. In each process, the irradiation time is fixed at different energies (Table 1) to obtain different nanosized sizes in each sample.

Table 1. Preparation parameter

Sample No.	Laser Energy (J)	Laser Pulse (PS)	Ablation Time (SEC)
1	400	100	30
3	800	100	30

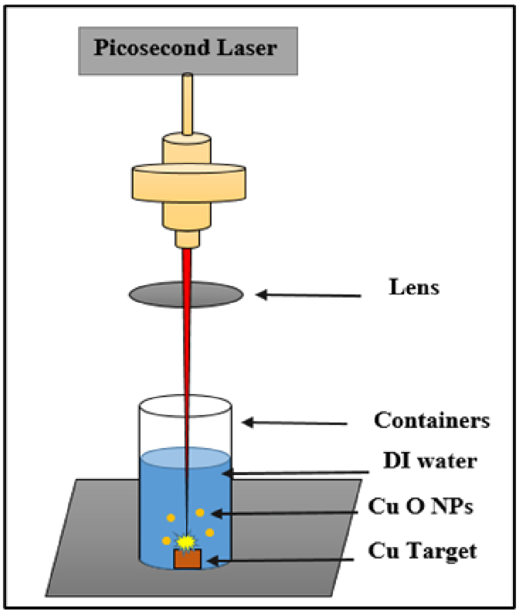

Figure 1. Diagrammatic representation of synthesis strategy of CuO NPs using PLAL

3. RESULTS AND DISCUSSION

3.1 UV-visible analysis

UV-Visible spectroscopy is widely employed for studying how nanoparticles act with light in the ultraviolet and visible regions. It makes use of the fact that electrons in nanoparticles absorb light and change from a lower to a higher energy state, predominantly from a valence band to a conduction band. The optical transitions in CuO nanoparticles are shaped by size, shape, and quantum confinement, all of which lead to changes in the peaks seen in absorption. Therefore, UV-Vis analysis is important since it supplies useful information about band gap energy, particle size, and the extent of particle agglomeration.

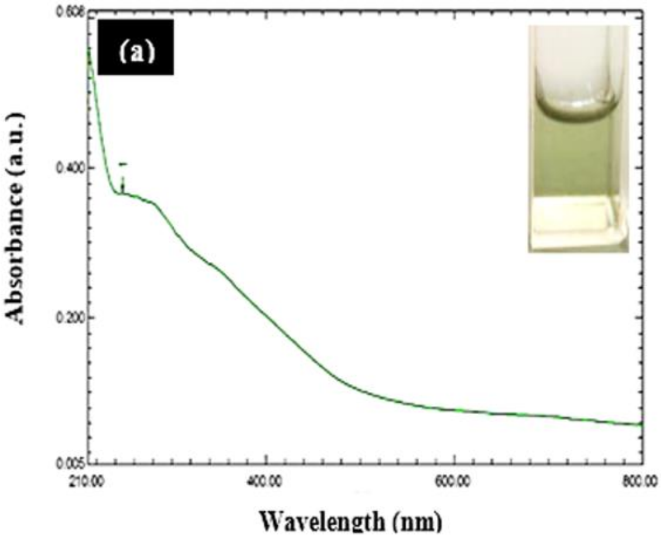

(a) 400 J

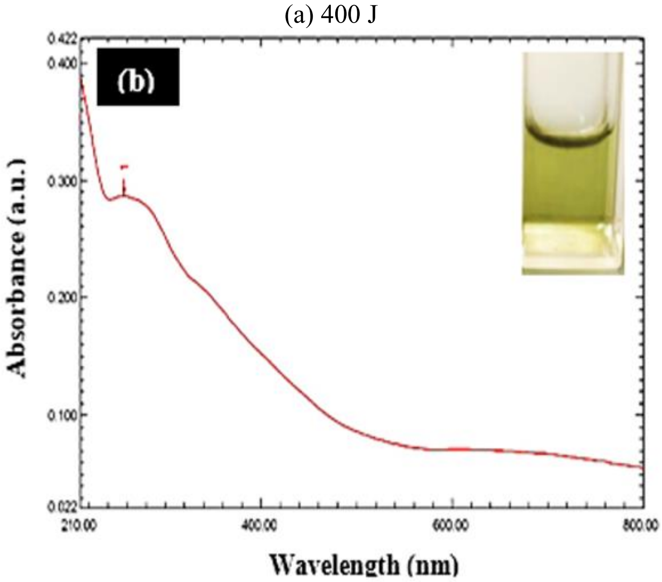

(b) 800 J

Figure 2. UV-visible absorption spectra of CuO nanoparticle colloids NPs

Studying the optical ABS of the prepared suspicion is of great interest due to its valuable scientific meaning. The optical ABS spectra depend on the crystalline structure of the prepared. Figure 2 depicts an effect of various preparation parameters on the ABS spectra. The ABS was examined in the ultraviolet and visible ranges the synthesized Cu NPs of the formed colloid were examined by optical and structural techniques. UV-visible absorption spectra of CuO nanoparticle colloids in the range from (200 to 800) nm using UV-vis spectrophotometer (SP-3000 Plus, OPTIMA). CuO NPs were created by laser ablation of a Cu plate in DI water, and their UV-visible absorption spectra were examined as a function of laser energy (400 and 800 mJ) and ablation time (30 min).

From Figure 2(a), the sample shows absorption at around 210 this is ascribed to electron transitions in copper oxide from a valence band to a conduction band, which are a hallmark of metal oxides because of nanoscale quantum confinement effects and a comparatively weaker band at around 600 nm this represents absorption in the visible light spectrum, which is equivalent to the CuO band gap (~1.4 eV). The size and dispersion of the nanoparticles are seen by this peak [36, 37]. From Figure 2(b), the sample shows absorption at around 650 nm and also demonstrated a redshift with an increasing in laser energy, which was an increasing in particle size This redshift indicates (1) a larger size of nanoparticles. Mie theory states that light at longer wavelengths (redshift) is absorbed by bigger particles. (2) Modifications to the morphology or crystal structure: Particles at 800 mJ were larger and more aggregated (elongated nanoflakes), according to SEM images. (3) Higher laser energy has the effect of increasing the copper target's rate of vaporization, which results in the creation of bigger nanoparticles. It was observed that the optical absorption characteristics of NPs colloids prepared at various energies were not very much different which can be due to the morphological resemblance [38, 39].

3.2 XRD analysis

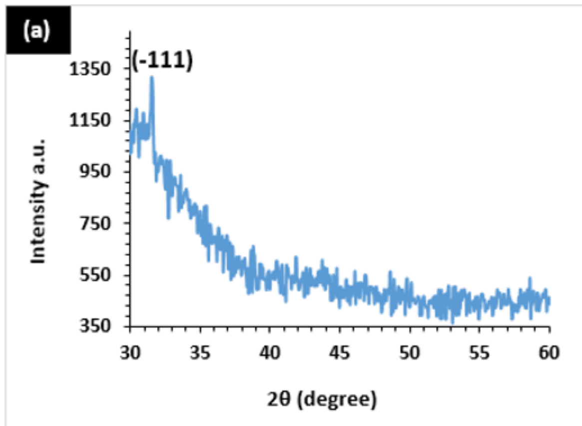

(a) 400J

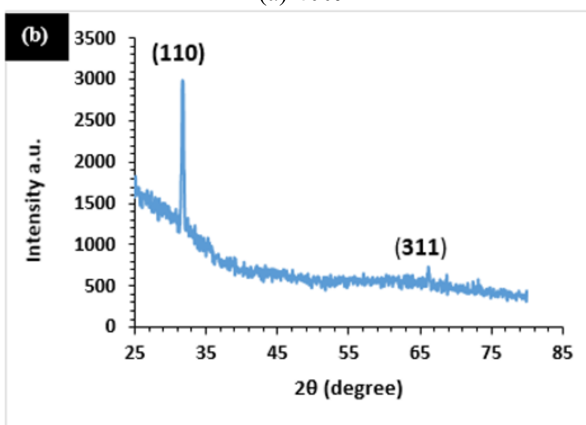

(b) 800J

Figure 3. XRD spectrum for CuO NPs synthesized at laser energy in DI for 30 min with laser pulse 100 PS

Figure 3 illustrates Crystal structure and particle size of CuO nanoparticles obtained by PLAL of copper at two different energy densities (400 mJ and 800 mJ) were measured by XRD.

The CuO nanoparticles formed at 400 J are illustrated in Figure 3(a). XRD spectrum of CuO nanoparticles exhibits two dominantly intense peaks at 34.626° and 34.714° 2θ respectively which belong to the (-111) monocline plane of CuO. The lack of other copper planes at 2θ = 34.714° is probably due to low CuO concentration. In Figure 3(b), CuO nanoparticles synthesized at 800 mJ energy level is illustrated. For CuO nanoparticles, the XRD spectrum exhibits two intense peaks at 2θ values of 31.49° and 66.45° for the monoclinic crystal phase of copper oxide and the (311) plane of copper oxide, respectively, compared with JCPDS data (48-1548). XRD analysis for the NP samples revealed that there is copper oxide present in the samples. This consequence correlates well with the UV-visible absorption measurements as reported earlier [40].

Table 2 provides a quantitative analysis of XRD data using the following Scherrer's Eq. (1) to estimate particle size.

Table 2. Identification of XRD parameters for CuO NPs

Ablation Condition	2θ (°)	Orientation (hkl)	FWHM (°)	d-spacing (A°)	Particle Size	Matched by
400J 30 min	34.626	-111	1.00	2.58848	30.2	JCPDS data (48-1548)
	34.714		1.00	2.58848	32.4	JCPDS data (48-1548)
800 J 30 min	31.7296	110	0.2952	2.82014	45.7	JCPDS data (48-1548)
	66.2359	311	0.2952	1.41103	74.2	JCPDS data (48-1548)

$$D = \frac{K\lambda}{\beta \cos\theta} \quad (1)$$

where, λ stands for the X-ray wavelength (Cu-Kα ≈ 0.154 nm), β stands for a full width at half maximum (FWHM) in radians, θ is the diffraction angle, and D stands for a crystallite size (nm).

3.3 SEM analysis

Figure 4 illustrates the SEM images of CuO NPs, produced at 800 mJ laser energies for 30 min ablation time with different magnifications. The nanoparticles appear elongated, with a structure that looks like nanoflakes, which is common for CuO NPs prepared by laser ablation in liquids. The particles seem to have sharp edges and a relatively uniform directionality in their growth. The image shows significant aggregation of nanoparticles, due to the high-energy environment and the reactivity of freshly formed nanoparticles.

The surface of the particles seems rough, which can increase surface area, potentially enhancing the catalytic properties of the CuO NPs. CuO nanoparticles with an elongated nanoflake structure and a rough surface are much more effective as catalysts. With these surface features, the surface-to-volume ratio rises, so there are more active locations for chemical reactions. The rough texture makes the nanoparticles both absorb more light and separate electrons and holes more effectively, which aids photocatalysis and antibacterial action. Also indicative of rapid cooling and solidification following laser ablation.

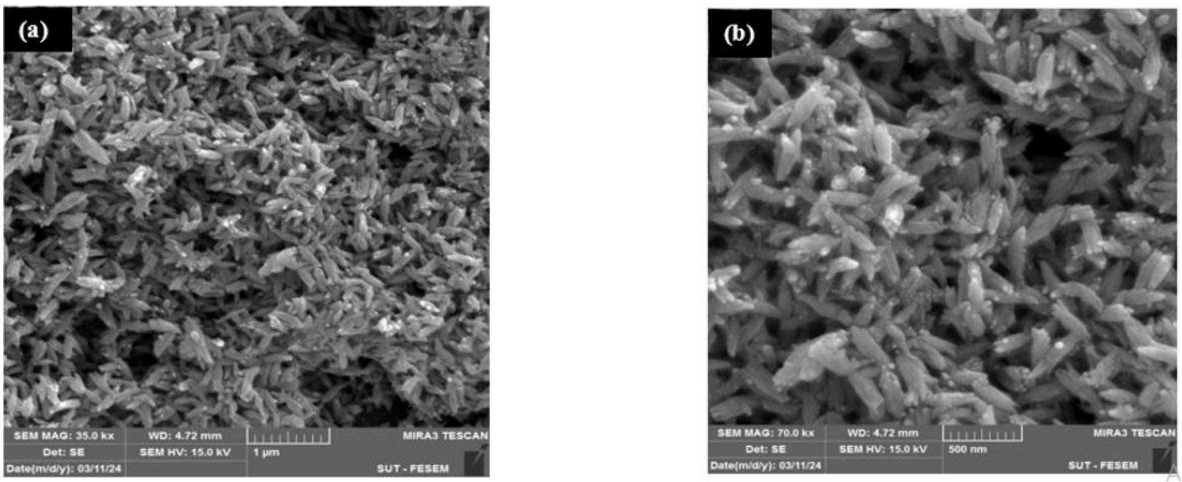

(a) 1µm (b) 500nm

Figure 4. SEM image for CuO NPs prepared by PLAL at laser energy 800mJ and ablation time 30min at (a) 1µm and (b) 500 nm magnification

4. CONCLUSION

In the work, copper oxide nanoparticles (CuO NPs) were produced with PLAL at two energy levels, 400 mJ and 800 mJ. As laser energy raised, UV-visible spectroscopy registered redshifts in the absorption spectra, meaning the particles became larger. XRD tests confirmed that the particles adopted a monoclinic structure and had an average size from 30 to 74 nm. By looking at the SEM images, we found that higher laser power formed longer, flake-like particles with rough surfaces that could help with catalysis. Because of their useful morphology and optical properties, CuO NPs from PLAL are considered promising for photocatalysis, antibacterial purposes, and biomedicine. It is shown by the results that laser ablation with varying power changes the properties of nanoparticles for particular uses.

REFERENCES

[1] Sadrolhosseini, A.R., Noor, A.S.B.M., Shameli, K., Mamdoohi, G., Moksin, M.M., Adzir Mahdi, M. (2013). Laser ablation synthesis and optical properties of copper nanoparticles. Journal of Materials Research, 28(18): 2629-2636. https://doi.org/10.1557/jmr.2013.244

[2] Ha, H., Müller, S., Baumann, R.P., Hwang, B. (2022). Peakforce quantitative nanomechanical mapping for surface energy characterization on the nanoscale: A mini-review. Facta Universitatis, Series: Mechanical Engineering, 22(1): 1-12. https://doi.org/10.22190/FUME221126001H

[3] Novotný, K., Krempl, I., Afonin, I., Prokeš, L., Vaňhara, P., Havel, J. (2025). Laser-induced plasma spectroscopy in pulsed laser ablation synthesis of nanoparticles in liquid. Talanta, 290: 127767.

[4] Aziz, A.A., Khalid, E.A., Alwan, A. S. (2020). Effect of Nd-Yag laser pulses on mechanical properties of carbontriding steel type (AISI 1006). Journal of Mechanical Engineering Research and Developments, 43(5): 80-88.

[5] Ajaj, K., Al-Jubbori, M.A., Ali, A.M. (2023). Influence of ultraviolet irradiation on the optical properties and biological activity of copper nanoparticles prepared by pulsed laser ablation. Journal of Laser Applications, 35(4). https://doi.org/10.2351/7.0001221

[6] Jaber, G.S., Dhaif, S.S., Abdul Hussian, T.A., Ibrahim, N.A., Arifiyanto, A. (2024). Corrigendum to "Enhancing the prodigiosin pigment by adding Ag\TiO2 synergism for antibacterial activity" [Biocatal. Agric. Biotechnol. 54 (2023) 1–8]. Biocatalysis and Agricultural Biotechnology, 58: 103227. https://doi.org/10.1016/j.bcab.2024.103227

[7] Alhajj, M., Safwan Abd Aziz, M., Salim, A.A., Sharma, S., Kamaruddin, W.H.A., Ghoshal, S.K. (2023). Customization of structure, morphology and optical characteristics of silver and copper nanoparticles: Role of laser fluence tuning. Applied Surface Science, 614: 156176. https://doi.org/10.1016/j.apsusc.2022.156176

[8] Khalid, A., Jaber, G.S., Dhaif, S.S. (2023). Preparation of TiO2NPs by laser and study its antibacterial activity against bacterial pathogens. In AIP Conference Proceedings, 2977(1): 040055. https://doi.org/10.1063/5.0183601

[9] Alwan, A.S., Khalid, E.A., Jaddoa, A.A. (2020). Improvement the corrosion behavior and wear characteristics of AISI 304 stainless steel by using Nd-Yag laser surface treatment. Journal of Mechanical Engineering Research, 43(4): 50-59.

[10] Kareem, M.M. (2019). The Effect of laser shots on morphological and optical properties of copper oxide NPs prepared by Nd-Yag laser of 1064 nm wavelengths in distilled water. Passer Journal of Basic and Applied Sciences, 3(2): 200-206. https://doi.org/10.24271/psr.33

[11] Adnan, N.N., Ab Razak, S.N., Roslan, M.S., Taib, N.A.M., Nurhafizah, H., Amran, N.B. (2020). Pulsed laser ablation produced copper nanoparticles (CUO NPS): The influence of time. Solid State Phenomena, 307: 279-284. https://doi.org/10.4028/www.scientific.net/ssp.307.279

[12] Jaber, G.S., Khashan, K.S., Abbas, M.J. (2021). Study the antibacterial activity of zinc oxide nanoparticles synthesis by laser ablation in liquid. Materials Today: Proceedings, 42: 2668-2673. https://doi.org/10.1016/j.matpr.2020.12.646

[13] Alwan, A.M., Mohammed, M.S., Shehab, R.M. (2020). Optimizing plasmonic characteristics of Ag-AuNPs/Nanohillocks Si heterostructures for efficient SERS performance. International Journal of Nanoelectronics & Materials, 13(2): 323-340.

[14] Alwan, A.M., Mohammed, M.S., Shehab, R.M. (2020). Modified laser-etched silicon covered with bimetallic Ag–Au Alloy nanoparticles for high-performance SERS: Laser wavelength dependence. Indian Journal of Physics, 95(9): 1843-1851. https://doi.org/10.1007/s12648-020-01845-w

[15] Mohammed, S.A.A., Khashan, K.S., Jabir, M.S., Abdulameer, F.A., Sulaiman, G.M., Al-Omar, M.S., Mohammed, H.A., Hadi, A.A., Khan, R.A. (2022). Copper oxide nanoparticle - decorated carbon nanoparticle composite colloidal preparation through laser ablation for antimicrobial and antiproliferative actions against breast cancer cell line, MCF-7. BioMed Research International. https://doi.org/10.1155/2022/9863616

[16] Shehab, R.M., Alwan, A.M. (2024). Improved the sensitivity and limit of detection of surface alloying SERS sensors by controlling the mixing ratio of trimetallic (Ag-Au-Pd) nanoparticles. International Journal of Nanoelectronics and Materials (IJNeaM), 16(2): 359-370. https://doi.org/10.58915/ijneam.v16i2.1234

[17] shehab, R.M., Alwan, A.M. (2015). Characterization of (nanostructures Silver/Silicon nano porous) active substrates for surface enhanced RAMAN scattering (SERS) as a function to porous silicon parameters. Engineering and Technology Journal, 33(3B): 556-563. https://doi.org/10.30684/etj.33.3b.15

[18] Husham, K.A.F., Khdier, H.M., Saadoon, N.M., Ahmed, A.M. (2024). Preparation of CuO/PVA nanocomposite thin films for gamma ray attenuation via PLA method. Journal of Nanostructures, 14(3): 712-722.

[19] Hassan, E.H., Ali, A.H., Shehab, R.M., Alrida, W.A.A., Mahdi, M.S. (2023). Using K-mean clustering to classify the kidney images. Iraqi Journal of Science, 64(4): 2070-2084. https://doi.org/10.24996/ijs.2023.64.4.41

[20] Hassan, E.H., Ali, A.H., Shehab, R.M., Mahdi, M.S., Abd Alrida, W.A. (2023). Mask laws to study texture features of the kidney infection. Iraqi Journal of Science, 64(5): 2261-2270. https://doi.org/10.24996/ijs.2023.64.5.14

[21] Jaber, G.S., khashan, K.S., Abbas, M.J., Ibrahim, N.A. (2023). Improvement of glass ionomer restoration by adding ZnO nanoparticles prepared by laser in (Vitro study). Journal of the Indian Chemical Society, 100(2): 100879. https://doi.org/10.1016/j.jics.2023.100879

[22] Majed, A.A., Khalid, G.A., Humadi, A.F. (2024). Portable uroflowmetry system with integrated software for home urinary monitoring. In 2024 International Conference on Electrical and Computer Engineering Researches (ICECER), Gaborone, Botswana, pp. 1-5. https://doi.org/10.1109/icecer62944.2024.10920439

[23] Kudhur, A.Y., Salim, E.T., Kara, I., Fakhri, M.A., Mahdi, R.O. (2023). Structural optical and morphological properties of copper oxide nanoparticles ablated using pulsed laser ablation in liquid. Journal of Optics, 53(3): 1936-1945. https://doi.org/10.1007/s12596-023-01331-6

[24] Fouad, N., Mahmoud, A., Abdel Samad, F., El-Salam, Y. A., Ashour, M., Apsari, R., Mohamed, T. (2024). Utilizing the 2nd harmonic Nd: YAG laser ablation in liquid for the production of copper oxide quantum dots: Influence of laser fluence and ablation duration. Physica B: Condensed Matter, 694: 416453. https://doi.org/10.1016/j.physb.2024.416453

[25] Mohammad, R.S., Aldlemy, M.S., Ahmed, A.M., Falah, M.W., Ahammed, S.J., Yaseen, Z.M. (2025). Thermal analysis of graphene-based nanofluids for energy system and economic feasibility. Journal of Nanomaterials, 2022: 3530419. https://doi.org/10.1155/2022/3530419

[26] Attallah, A.H., Abdulwahid, F.S., Ali, Y.A., Haider, A.J. (2023). Effect of liquid and laser parameters on fabrication of nanoparticles via pulsed laser ablation in liquid with their applications: A review. Plasmonics, 18(4): 1307-1323. https://doi.org/10.1007/s11468-023-01852-7

[27] Rashid, S.N., Jasim, A.S., Aadimb, K.A. (2022). Influence of number of pulses on characterization of nanoparticles of copper and its oxides synthesized by Nd: YAG laser ablation technique and its antibacterial activity. NeuroQuantology, 20(3): 150-159. http://dx.doi.org/10.14704/nq.2022.20.3.NQ22054

[28] Afan, H.A., Aldlemy, M.S., Ahmed, A.M., Jawad, A.H., Naser, M.H., Homod, R.Z., Mussa, Z.H., Abdulkadhim, A.H., Scholz, M., Yaseen, Z.M. (2022). Thermal and hydraulic performances of carbon and metallic oxides-based nanomaterials. Nanomaterials, 12(9): 1545. https://doi.org/10.3390/nano12091545

[29] Razaghianpour, M., Hantehzadeh, M.R., Sari, A.H., Darabi, E. (2021). Electric field assisted-laser ablation of cu nanoparticles in ethanol and investigation of their properties. Optical and Quantum Electronics, 54(1). https://doi.org/10.1007/s11082-021-03286-z

[30] Alwan, A.M., Mohammed, M.S., Shehab, R.M. (2020). The performance of plasmonic gold and silver nanoparticle-based SERS sensors. Iraqi Journal of Science, 61(6): 1320-1327. https://doi.org/10.24996/ijs.2020.61.6.10

[31] Tarasenka, N., Shustava, E., Butsen, A., Kuchmizhak, A. A., Pashayan, S., Kulinich, S.A., Tarasenko, N. (2021). Laser-assisted fabrication and modification of copper and zinc oxide nanostructures in liquids for photovoltaic applications. Applied Surface Science, 554: 149570. https://doi.org/10.1016/j.apsusc.2021.149570

[32] Shoeib, M.A., Abdelsalam, O.E., Khafagi, M.G., Hammam, R.E. (2012). Synthesis of Cu2O nanocrystallites and their adsorption and photocatalysis behavior. Advanced Powder Technology, 23(3): 298-304. https://doi.org/10.1016/j.apt.2011.04.001

[33] Goncharova, D.A., Lapin, I.N., Savelyev, E.S., Svetlichnyi, V.A. (2017). Structure and properties of nanoparticles fabricated by laser ablation of bulk metal copper targets in water and ethanol. Russian Physics Journal, 60(7): 1197-1205. https://doi.org/10.1007/s11182-017-1195-3

[34] Swarnkar, R.K., Singh, S.C., Gopal, R. (2011). Effect of aging on copper nanoparticles synthesized by pulsed laser ablation in water: Structural and optical characterizations. Bulletin of Materials Science, 34(7): 1363-1369. https://doi.org/10.1007/s12034-011-0329-4

[35] Beck, R.J., Bitharas, I., Hand, D.P., Maisey, T., et al. (2020). Dynamics of picosecond laser ablation for surgical treatment of colorectal cancer. Scientific Reports, 10(1): 20261.

[36] Khalid, G.A., Abdulmawjod, M.I., Al-Bayaty, A. (2024). A comprehensive analysis of respiratory patterns and physiological parameters in asthma, bronchitis, and croup. Electrical Engineering Technical Journal, 1(1): 35-49. https://doi.org/10.51173/eetj.v1i1.3

[37] Dizajghorbani Aghdam, H., Azadi, H., Esmaeilzadeh, M., Moemen Bellah, S., Malekfar, R. (2019). Ablation time and laser fluence impacts on the composition, morphology and optical properties of copper oxide nanoparticles. Optical Materials, 91: 433-438. https://doi.org/10.1016/j.optmat.2019.03.027

[38] Collier, A.M., Louwagie, E., Khalid, G.A., Jones, M.D., Myers, K., Jerusalem, A. (2024). Effects of fetal position on the loading of the fetal brain during the onset of the second stage of labor. Journal of Biomechanical Engineering, 146(11): 111001. https://doi.org/10.1115/1.4065557

[39] Alwan, A.M., Mohammed, M.S., Shehab, R.M. (2020). Optimization of an ultra-sensitive Ag core-Au shell nanoparticle/Si Surface-enhanced Raman scattering (SERS) sensor. AIP Conference Proceedings, 2307: 020005. https://doi.org/10.1063/5.0032762

[40] Fernández-Arias, M., Boutinguiza, M., del Val, J., Riveiro, A., Rodríguez, D., Arias-González, F., Gil, J., Pou, J. (2020). Fabrication and deposition of copper and copper oxide nanoparticles by laser ablation in open air. Nanomaterials, 10(2): 300. https://doi.org/10.3390/nano10020300